Atmospheric Research 245 (2020) 105056

Contents lists available at ScienceDirect

Atmospheric Research

journal homepage: www.elsevier.com/locate/atmosres

Invited review article

The development and application of satellite remote sensing for atmospheric compositions in China

Xingying Zhang[a,*], Fu Wang[a], Weihe Wang[a], Fuxiang Huang[a], Binglong Chen[a], Ling Gao[a], Shupeng Wang[a], Huanhuan Yan[a], Hanhan Ye[b], Fuqi Si[b], Jin Hong[b], Xiaoying Li[c], Qiong Cao[d], Huizheng Che[e], Zhengqiang Li[c]

[a] Key Laboratory of Radiometric Calibration and Validation for Environmental Satellites (LRCVES/CMA), National Satellite Meteorological Center, China Meteorological Administration (NSMC/CMA), Beijing 100081, China
[b] Key Laboratory of Optical Calibration and Characterization, Anhui Institute of Optics and Fine Mechanics, Chinese Academy of Sciences, Hefei 230031, China
[c] State Key Laboratory of Remote Sensing Science, Aerospace Information Research Institute, CAS, Beijing 100101, China
[d] Shanghai Institute of Satellite Engineering, Shanghai 201109, China
[e] Chinese Academy of Meteorological Sciences, China Meteorological Administration (CAMS/CMA), Beijing 100081, China

ARTICLE INFO

Keywords:
Atmospheric composition
Chinese satellite missions
Remote sensing
Trace gases
Greenhouse gases
Aerosol

ABSTRACT

The variations of atmospheric compositions (ACs) can change the atmospheric interactions with other parts of the ecosystem, and it also affects the energy budget of the Earth. Satellite remote sensing plays a crucial role in monitoring AC by providing a matchless global perspective with consistency over long periods. Although China started space exploration missions in the early 1970s, the situation of lacking operational AC satellite missions was turned around until the launch of FY-3A in 2008. In the following decade, more Chinese pathfinder AC satellite missions were putting into operation, and then lead to a boom in related researches on air quality, trace gases and greenhouse gases (GHG) measurements. In particular, moderate resolution imageries of polar mission FY-3 series are used to monitor air quality, and recent comparable imagery onboard geostationary mission FY-4A could provide similar air pollution observation with higher temporal resolution of up to five minutes. Nadir spectrographs onboard FY-3 series and the latest pathfinder mission GF-5 aims to monitor various trace gases. Moreover, hyper-spectrometers onboard GF-5 and another pathfinder mission TanSat are devoted to mapping the global distribution of GHG, as a supplement to operational mission FY-3D. Besides the progress in the space-borne part, the in-situ calibration and validation have achieved fruitfully since the late 1990s, gaining insight into the consistency between the satellite and in-situ observations over China. Applications and studies based on Chinese satellite missions are still growing since it has only been a few years after their launch. Furthermore, the newly planned missions for monitoring AC with active remote sensing instruments are also illustrated, such as lidar, which will be able to improve the accuracy of space-borne observations.

1. Introduction

The composition of atmosphere plays a significant role in the earth's ecosystems since it involves in the interactions between the atmosphere and other spheres (Betts et al., 1996). Emissions from human activities have been changing atmopseheric compositions (ACs) more significantly since the industrial revolution, especially in the era of global modernization. In particular, halocarbon emissions involved in chemical reactions have led to an ozone-depleted region in the southern polar region, known as the “ozone hole” (Liang et al., 2017; Newman et al., 1995). Emissions of nitrogen oxides could participate in photo-catalytic reactions and generate ozone and photochemical smog in the troposphere (Crutzen, 1979). Emissions of acidic gases such as sulfur dioxide (SO_2), nitrogen dioxide (NO_2) and carbon dioxide (CO_2) can lead to the destruction of the biosphere by forming acid rain (Singh and Agrawal, 2007). Various types of aerosol emitted by automobile, urban construction and food cooking lead to changes in both air quality and the earth's radiation balance (Lacis et al., 1992). The rapid increase of greenhouse gases (GHG), including CO_2 and methane, causes global warming due to their strong absorption on surface infrared radiation and leads to a series of related environmental issues such as glacier melting, higher snowline and sea-level rise (Manabe and Wetherald, 1980).

* Corresponding author.
E-mail address: zxy@cma.gov.cn (X. Zhang).

https://doi.org/10.1016/j.atmosres.2020.105056
Received 24 March 2020; Received in revised form 17 May 2020; Accepted 18 May 2020
Available online 20 May 2020

In the early 1970s, the launch of meteorological satellites marked the beginning of a new era for the observation of global atmopseheric compositions (ACs). Advanced Very High Resolution Radiometers (AVHRRs) were the initial payloads onboard National Oceanic and Atmospheric (NOAA) polar satellite series for atmospheric aerosol detection (Zhang et al., 2015), followed by more advanced instruments onboard later American and European missions, such as Moderate-resolution Imaging Spectroradiometer (MODIS) (Salomonson et al., 1989), Multi-angle Imaging Spectroradiometer (MISR) (Diner et al., 1989), Polarization and Directionality of the Earth's Reflectances (POLDER) (Bréon et al., 2002), Cloud-Aerosol Lidar with Orthogonal Polarization(CALIOP) (Winker and Pelon, 2003), and Visible Infrared Imaging Radiometer (VIIRS) (Hutchison and Cracknell, 2006). The instruments using UV-light bands to probe the atmospheric column are sensitive to trace gas concentrations. Such sensors like Total Ozone Mapping Spectrometer (TOMS) and Solar Backscatter Ultraviolet (SBUV) series (Heath et al., 1975; Herman et al., 1991), Global Ozone Monitoring Experiment (GOME) series(Burrows et al., 1999), Scanning Imaging Absorption spectroMeter for Atmospheric CHartographY (SCIAMACHY) (Bovensmann et al., 1999), Ozone Monitoring Instrument (OMI) (Dobber et al., 2006), Ozone Mapping and Profiler Suite (OMPS) (Flynn et al., 2014) were deployed to provide deep insight into atmospheric chemistry, especially ozone, sulfur dioxide, nitrogen dioxide, even formaldehyde (CH_2O), glyoxal ($C_2H_2O_2$), bromine monoxide (BrO), iodine monoxide (IO), and chlorine dioxide (ClO_2) (Abad et al., 2019). Other instruments such as TANSO-FTS/GOSAT (Thermal And Near-infrared Sensor for carbon Observation - Fourier Transform Spectrometers / Greenhouse gases Observing Satellite), TANSO-FTS-2/GOSAT-2, and spectrometry onboard OCO-2/OCO-3 (Orbiting Carbon Observatory-2/Observatory-3), aimed to provide a global map of CO_2 (O'Dell et al., 2012; Taylor et al., 2012; Nakajima et al., 2012; Eldering et al., 2019). Due to advanced spatio-temporal and spectral sampling capabilities, the latest European mission TROPOspheric Monitoring Instruments (TROPOMIs) on Sentinal-5 Precursor (Sentinal-5P) and its successor Sentinel-5 can map tropospheric/stratospheric trace gases, GHG, along with cloud and aerosol parameters with even higher accuracy (Veefkind et al., 2012). For extension of the polar European mission, future geostationary Sentinal-4 instruments are planned to obtain regular information of trace gases and aerosol on minutely timescale (Gulde et al., 2017). At present advanced multi-spectral imagers onboard geostationary platforms, like AHI/H8 and ABI/GOES-R, are already capable of providing minutely aerosol observation for air quality detection (Ignatov et al., 2016).

Before China initiated the meteorological satellite program in the 1970s, a few of preliminary researches which concerned atmospheric conditions were carried out using foreign meteorological satellite data (Zeng, 1974). After decades of development, two generations of meteorological satellites, polar-orbiting series (FY-1, FY-3) and geostationary series (FY-2, FY-4), have been put into operation. Nevertheless, the first generation of Chinese meteorological satellites was in lack of capability other than the detection of atmospheric conditions. However, the second-generation polar satellite FY-3A, launched in 2008, marked a milestone in monitoring AC for Chinese meteorological satellite program (Dong et al., 2009; Zhang et al., 2009a; Yang et al., 2009). Since then, steady progress had resulted in enhanced capabilities of new instruments onboard Fengyun series in the following decades (), Gaofen series (Hazem, 2019) and TANsat mission Liu et al., 2018). Meanwhile, during these years significant progress on retrieval algorithms and validation of satellite observation using in-situ measurements had been achieved as well.

This paper aims to provide a review of Chinese space-borne remote sensing programs concerning AC and their contribution to the understanding of global changes. The remainder of this paper is organized as follows. Section 2 describes the evolution of instruments and technological advancements, and focuses on the missions of exploiting aerosol, trace gas, greenhouse gas, validation of satellite observations and data applications. Section 3 takes a glance at the Chinese future plans of space-borne observations on AC, including the limitations and challenges of these missions. Section 4 presents our conclusions and a series of recommendations for the future.

2. Status of Chinese satellite observation on atmospheric composition

2.1. Chinese satellite missions related to atmospheric composition

The Chinese space programs initiated in the 1960s. Among those, meteorological satellites were the very first which got approval from the Chinese government. Then after decades of development, the first generation of Fengyun satellite series was launched. In particular, the polar meteorological satellites, namely Fengyun 1 (FY-1) series, was launched in the 1980s, while the geostationary meteorological satellites, known as Fengyun 2 (FY-2) series, were put into operation in the late 20th century (Zhang, 2001; Wang et al., 2011). Till then, both polar and geostationary meteorological satellite series had been established by China (Zhang et al., 2019a). Other satellite missions, such as the satellite series aimed for applications of land resources, oceans, and environmental protection, have been put into practice during the same time (Pan, 2003; Guo et al., 2005; Xu et al., 2011). To be specific, satellite series for land resource monitoring were known as the China-Brazil Earth Resources Satellite (CBERS) program. Its first satellite, CBERS-01, was launched in 1999, which also represented an example of international cooperation between China and Brazil (Guo et al., 2005). Furthermore, satellite series for oceanic water-colour monitoring, named Haiyang-1 (HY-1), was launched in 2002 (Sun, 2003). The one for environmental protection, namely Huanjing-1 (HJ-1) mini-satellite constellation, was put into effect as early as 2003 (Wang et al., 2005). The spatio-temporal and spectral resolutions of the instruments have been improving in those years, while the ground segment has been implemented and applications have been continuously expanded (Hu et al., 2001; Asher et al., 2019).

After years of effort, the second generation of Chinese polar orbit meteorological satellites, Fengyun 3 (FY-3), were successfully launched starting from 2008. The first satellite of the FY-3 series, known as FY-3A, has turned over a new chapter in the history of Chinese space-borne missions for AC detection. There are 11 instruments onboard FY-3A compared with the single payload of the FY-1 series (Huang et al., 2008). One of the primary instruments, namely Medium Resolution Spectral Imager (MERSI), is a 20-channel radiometer covering visible, short-wave and long-wave infrared bands (Dong et al., 2009). Detection of water vapor is one of MERSI's typical applications to quantitatively understanding atmospheric constituent (Gong et al., 2018; Gong et al., 2019; Wang et al., 2013). MERSI is also the first Chinese remote sensing satellite capable of monitoring global atmospheric aerosol on daily basis, and its product has been used for detection of dust (Bao et al., 2019). Moreover, other two UV spectro-radiometers, namely Total Ozone Unit (TOU) and Solar Backscatter Ultraviolet Sounder (SBUS), can measure total ozone amount and ozone profile, respectively (Zhang et al., 2009a; Zhang et al., 2007). MERSI, TOU, and SBUS are also equipped on FY-3B/C, while FY-3D launched in November 2017 has upgraded with enhanced MERSI-II and a new payload known as Greenhouse-gases Absorption Spectrometer (GAS) aimed for monitoring CO_2, CH_4, CO, and N_2O (Lu et al., 2019; Zhang et al., 2019b). Later, in 2016, the second generation of Chinese geostationary meteorological satellites, Fengyun-4A (FY-4A), was launched successfully. The advanced multi-spectral imager onboard FY-4A, known as Advanced Geosynchronous Radiation Imager (AGRI), has the similar bands with instruments onboard the polar platform, such as MODIS and MERSI (Zhang et al., 2019a), so AGRI data can apply the similar algorithms of aerosol optical depth retrieval. Those applications using geostationary data with temporal resolution up to 5 min have much potential in air quality monitoring and modeling (Saide et al., 2014).

Before GAS/FY-3D, the Chinese Carbon Dioxide Observation Satellite, also known as TanSat ("Tan" means carbon in Chinese), was successfully launched in December 2016. The project was dedicated to monitoring CO_2 with two primary payloads, Atmospheric Carbon-dioxide Grating Spectroradiometer (ACGS) and Cloud and Aerosol Polarization Imager (CAPI) (Yang et al., 2018). Furthermore, most recently the Gaofen-5 (GF-5) satellite as part of the China High-resolution Earth Observation System (CHEOS) mission was launched in May 2018. The instruments onboard GF-5 were specifying for detecting AC. For example, one instrument named Environment Monitoring Instrument is dedicated to monitoring trace gases and GHG, and the other one named Greenhouse Gas Monitoring Instrument (GMI) is aiming to measures CO_2 and methane. Besides, the Directional Polarization Camera (DPC) can provide more accurate aerosol measurements (Zhou et al., 2019). In addition, publications based on the above mentioned missions have provided us insights into the atmospheric composition and global distribution from the perspective of Chinese satellites.

2.2. Aerosol detection instruments and their applications

Detection of air pollution is one of the most important fields for applications of satellite remote sensing data. Imagers with visible bands can all be applied to aerosol optical depth retrieval algorithms. Charge Coupled Device (CCD) instrument onboard HJ-1 is a camera that includes four bands (430–520 nm, 520–600 nm, 630–690 nm and 760–900 nm) with 30 m spatial resolution (Sun et al., 2010b). Since the center wavelength of the first CCD band is close to the third band of MODIS and there is a linear relationship between these two, the aerosol optical depth (AOD) retrieval based on CCD and MODIS data has been established and validated (Wang et al., 2009; Wang et al., 2012a; Sun et al., 2010a; Li et al., 2012).

In addition, MERSI onboard FY-3 series is the first Chinese instrument applied for AOD retrieval (Zhang et al., 2009a). MERSI has 19 channels in VIS/NIR/SWIR (visible/near infrared/ short wave infrared red) bands and one in thermal IR band at 10.0–12.5 μm for FY-3A/FY-3B, while its upgraded version MERSI-II/FY-3D has 25 channels which are specified in Table 1. The spatial resolutions at nadir are 250 m for four VIS/NIR channels and one infrared channel, and 1 km for all other channels. The dark dense vegetation (DDV) algorithm was used for aerosol retrieval to provide global air quality information on a daily basis (Han et al., 2015; Ge et al., 2017). A pre-computed lookup table was established for a variety of geometry and aerosol conditions, then the products of aerosol optical properties, such as AOD (as illustrated in Fig. 1), were given for each pixel. This AOD product derived from FY-3/MERSI was comparable to those from MODIS (Tang et al., 2018; Xia et al., 2019) and was applied in dust storm monitoring (Mei et al., 2011) and surface PM2.5 retrieval (Zeng et al., 2017). Since AGRI/FY-4A had the corresponding channels for the dark target (DT) algorithm. The DT algorithm was applied to AGRI data and an AOD product (shown in Fig. 2) with high temporal resolution of up to 5 min was developed (; Zhang et al., 2019a).

Table 1
Specifications of MERSI, MERSI-II, AGRI HJ, DPC spectral bands for aerosol retrieval.

Payload	Channel	Central wavelength(μm)	Spatial resolution (m)
MERSI/MERSI-II	1	0.470	250
	2	0.550	250
	3	0.650	250
	20	2.13	1000
AGRI	1	0.470	1000
	2	0.650	500
HJ-1	1	0.475	30
DPC	1	0.443	3300
	2	0.490*	3300
	3	0.565	3300
	4	0.670*	3300
	5	0.763	3300
	6	0.765	3300
	7	0.865*	3300
	8	0.910	3300

* Polarized bands.

The recently deployed instrument, the DPC on board GF-5 is a multi-angle polarized sensor with three polarized bands (490 nm, 670 nm and 865 nm), five non-polarized bands (443 nm, 565 nm, 763 nm, 765 nm and 910 nm) and one dark band installed in a quickly rotating wheel. Since the polarimetric channels have three polarization directions (0°, 60° and 120°), the DPC can obtain continuous images over the same target from nine viewing angles (Li et al., 2018). An optimized AOD retrieval algorithm has been developed for DPC data, with further products such as Angstrom exponent and find-mode fraction (FMF) (Li et al., 2019b).

2.3. Trace gases monitoring instruments and their applications

There were totally four Chinese instruments capable of monitoring trace gases, including the Total Ozone Unit (TOU) and the Solar Backscatter Ultraviolet Sounder (SBUS) onboard FY-3 series, and the Environment Monitoring Instrument (EMI) and the Atmospheric Infrared Ultra-spectral Sounder (AIUS) equipped on GF-5 satellite.

TOU is the Chinese first space-borne atmospheric ozone monitoring instrument onboard FY-3A/B/C. As a single Ebert-Fastie spectrometer with a fixed grating and an array of exit slits, the detector of TOU is a Photo Multiplier Tube (PMT) measuring discrete wavelengths from 308.68 nm to 360.11 nm with a 1 nm bandwidth, which is specified in Table 2. TOU estimates the total column ozone from a pair of wavelengths of Huggins bands where ozone has relatively stronger absorption at one wavelength but weaker at the other (Dave and Mateer, 1967). The total column ozone for a given pixel is retrieved by the relation between the total column ozone and the difference of N-values in a pair of wavelengths (Wang et al., 2011). On this basis, the global ozone distribution was first mapped by TOU/FY-3A in late 2008 (Zhang et al., 2012). Since then, the FY-3 series has successfully monitored the multi-year variation of Antarctic ozone, as illustrated in Fig. 3. The TOU ozone products have been validated with both the ground-based dataset from the World Ozone and Ultraviolet Radiation Data Center (WOUDC) and the space-borne dataset from OMI/Aura daily product with Root Mean Square (RMS) differences of 4.3% and 3.1%, respectively (Wang et al., 2012b). Besides, TOU/FY-3A data has been used to monitor the total column ozone over the Arctic and has revealed a rapid declination starting from March 2011, with the monthly mean total column ozone 30% lower than the mean value observed during 1979–2010 (Zhang et al., 2012).

The other instrument onboard FY-3 series, SBUS, is a nadir-viewing sensor with double monochromators with three observation modes in orbit, namely earth mode, solar mode and internal lamp calibration mode. In earth mode, SBUS measures the backscattered ultraviolet radiation in the atmosphere at 12 discrete channels (specified in Table 2) in the 250–340 nm spectral region with 1.1 nm full-width half-maximum (FWHM) bandwidth, while solar irradiance of the same channels is weekly measured using solar mode. The ozone vertical profile retrieval algorithm of the SBUS is proved highly similar with the differences particularly in layers just above the tropopause where the ozone amounts often reach a maximum (Huang et al., 2008; Huang et al., 2010; Huang et al., 2012). This ozone-monitoring product derived from FY-3B SBUS is combined with NOAA SBUV/2 to monitor the severe ozone loss in the Arctic region from March to April 2011 (Liu et al., 2011), and also used to detect polar ozone depletion during the solar proton events (Huang et al., 2019).

The latest scientific pathfinder mission of China, namely GF-5, is equipped with two payloads EMI and AIUS to monitor trace gases. EMI is a nadir-viewing wide-field imaging spectrometer that has four spectral channels ranging from 240 nm to 710 nm with a spectral resolution

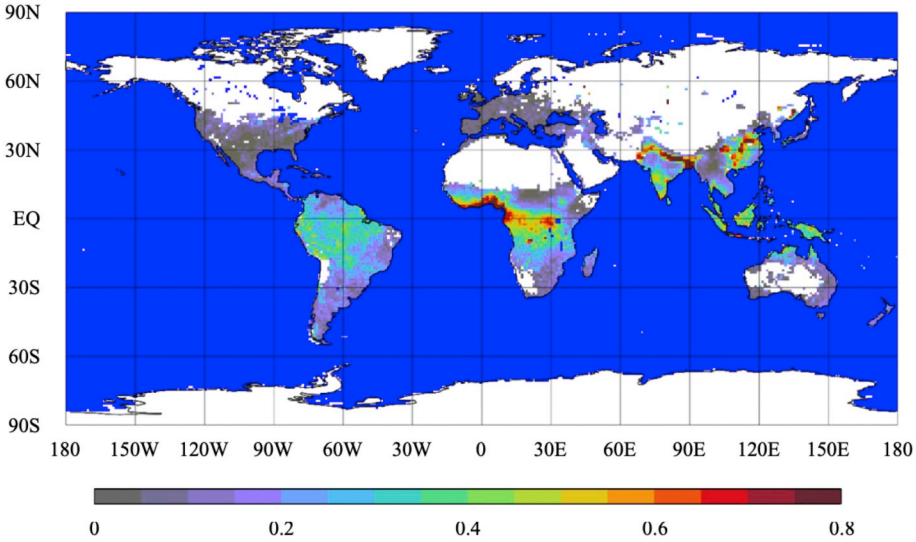

Fig. 1. Global distribution of terrestrial aerosol optical depth in January 2018 from FY-3D/MERSI-II. (Quoted from Yang et al., 2018).

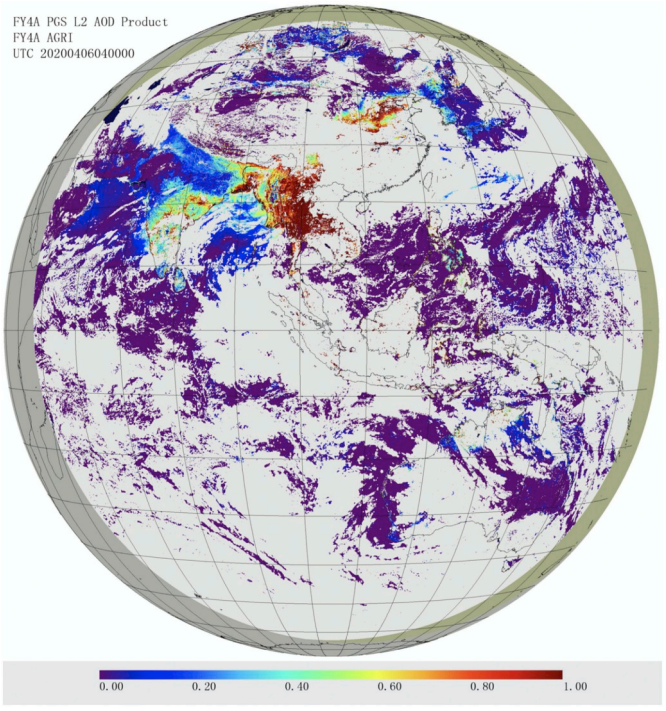

Fig. 2. Full disk distribution of terrestrial aerosol optical depth derived from FY-4A/AGRI at 0400 UTC on April 6th, 2020.

of 0.3–0.5 nm (as listed in Table 2). It aims to acquire global tropospheric and stratospheric trace gases (e.g., NO_2, O_3, CH_2O and SO_2) daily with its wide swath. The global map of ozone distribution acquired from EMI in October 2018 is demonstrated in Fig. 4. Besides, the EMI provides NO_2 monitoring product with better spatial resolution than OMI/Aura Mission and is comparable with TROPOMI/Sentinel-5P (as shown in Fig. 5). Moreover, AIUS is a Fourier transform infrared spectrometer (as specified in Table 2), also aims to measure ozone and other trace gases in the stratosphere and upper troposphere. Particularly, it could help understand the temporal variations of ozone in the Antarctic region. The previous studies have revealed that the relative difference was mostly within 10% (about 0.02–0.4 ppm) between 18 km and 58 km for the ozone retrieval, within 10% (0–0.5 ppm) between 15 km and 80 km for the H_2O retrieval, and within 10% (about

Table 2
Specifications of TOU/FY-3, SBUS/FY-3, EMI/GF-5 and AIUS/GF-5 spectral bands for trace gas monitoring.

Payload	Channel	Central wavelength(nm)	Bandwidth(nm)
TOU/FY-3	1	308.727	1.164
	2	312.638	1.152
	3	317.652	1.171
	4	322.464	1.156
	5	331.375	1.159
	6	360.253	1.140
SBUS/FY-3	1	252.00 ± 0.05	1 + 0.2
	2	273.62 ± 0.05	1 + 0.2
	3	283.10 ± 0.05	1 + 0.2
	4	287.70 ± 0.05	1 + 0.2
	5	292.29 ± 0.05	1 + 0.2
	6	297.59 ± 0.05	1 + 0.2
	7	301.97 ± 0.05	1 + 0.2
	8	305.87 ± 0.05	1 + 0.2
	9	312.57 ± 0.05	1 + 0.2
	10	317.56 ± 0.05	1 + 0.2
	11	331.26 ± 0.05	1 + 0.2
	12	339.89 ± 0.05	1 + 0.2
	Photometer	379.00 ± 1.00	3 + 0.3
EMI/GF-5	UV1	Range from 240 to 315	0.3–0.5*
	UV2	Range from 311 to 403	0.3–0.5*
	VIS1	Range from 401 to 550	0.3–0.5*
	VIS2	Range from 545 to 710	0.3–0.5*
AIUS/GF-5		Range from 750 to 4100 cm^{-1}	0.02 cm^{-1} *

* Spectral resolution.

0.1 ppb) between 30 km and 60 km for the HCl retrieval (Li et al., 2019c).

2.4. Greenhouse-gases monitoring instruments and their applications

ACGS is the main payload onboard TanSat, and it is the first space program aiming for mapping the global distribution of CO2, followed by GAS onboard FY-3D and GMI onboard GF-5. All these three instruments are hyper-spectrometers designed to measure SWIR back-scattered solar radiation. They all have O_2-A bands, but ACGS and GAS cover the weak and strong CO_2 absorption bands (1.61 μm and 2.04 μm). The 1.61 μm of CO_2 absorption band is mainly used for CO_2 concentration information collection, and the O_2-A and 2.04 μm bands are mainly used to correct interference that comes from the uncertainty of water vapor and aerosols (Liu et al., 2013; Liu et al., 2014; Wang et al., 2014). However, GMI chooses bands centered at 1.575 μm and

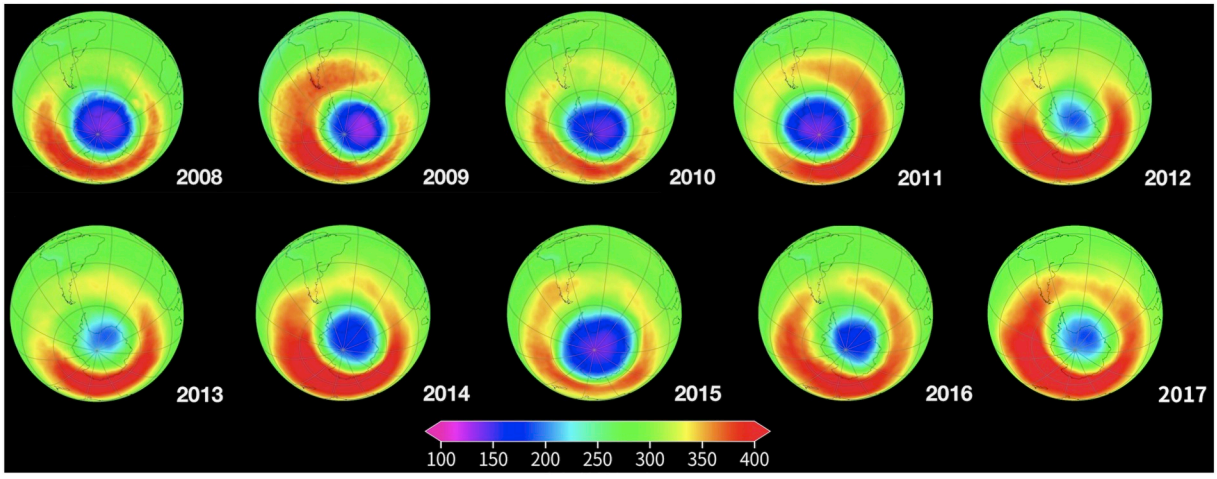

Fig. 3. Annual average of total ozone over the Antarctic region from 2008 to 2017. The colour represents the ozone thickness in Dobson units (DU).

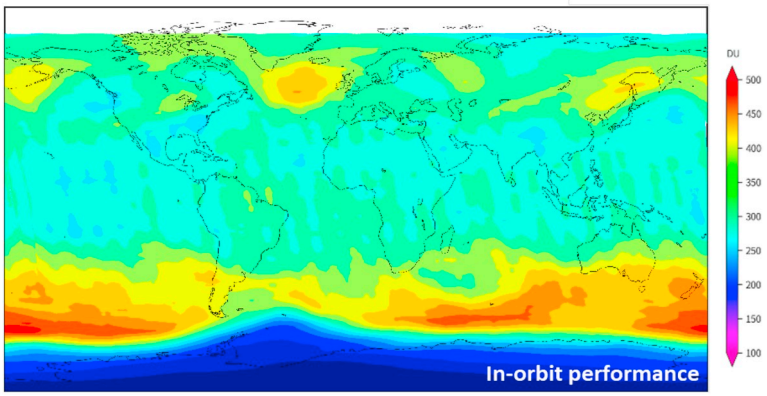

Fig. 4. Global monthly average of ozone total column distribution acquired from EMI in October 2018.

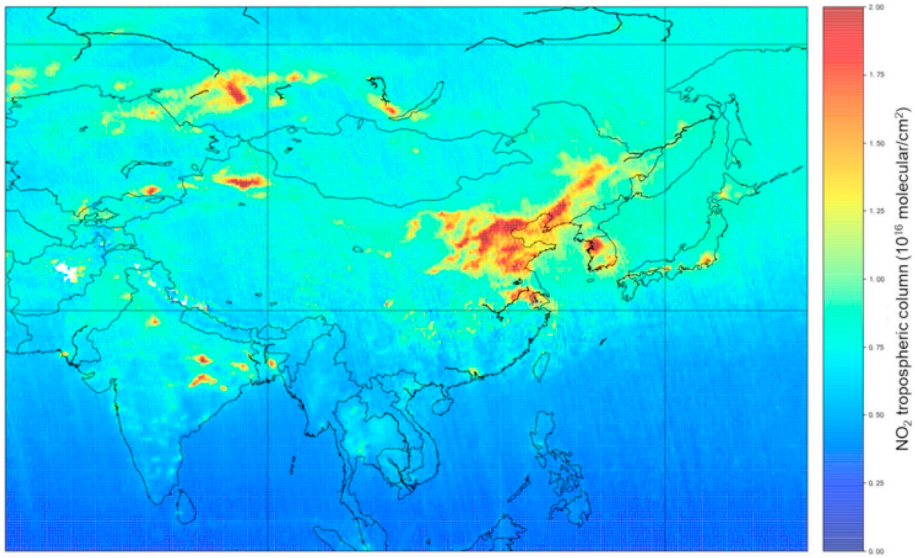

Fig. 5. Monthly average of tropospheric NO_2 columns over China and its surrounding countries acquired from EMI in February 2019.

2.05 μm for CO_2 retrieval, and the band centered at 1.65 μm for CH_4 (as shown in Table 3) (Xiong, 2018). GAS is also capable of monitoring CH_4 with its other band centered at 2.3 μm.

Preliminary TanSat XCO_2 product was verified against overlap measurement from OCO-2, and also has been validated against eight ground-based measurements, which reveal an average precision of 2.11 ppm (Liu et al., 2018). The GAS product has been generated by the operational system of the National Satellite Meteorological Center (NSMC) and delivered through the distribution system of FY-3 ground segments. Most recently, global distribution maps of CO_2 and CH_4 column concentration (as shown in Fig. 6) in September 2018 derived from GMI were published in Chinese (Xiong, 2019).

Table 3
Specification of ACGS/TanSat, GAS/FY-3D and GMI/GF-5 spectral bands for greenhouse gas monitoring.

Specification	ACGS/TanSat	GAS/FY-3D	GMI/GF-5
Bands(μm)	0.758–0.778	0.75–0.77	0.759–0.769
	1.594–1.624	1.56–1.72	1.568–1.583
	2.042–2.082	1.92–2.08	2.043–2.058
		2.20–2.38*	1.642-1.658*
Spectral resolution(μm) @1.6 μm	0.124	0.073	–
Spatial resolution(km)	2	13.2	–

* For CH_4 monitoring.

2.5. Ground-based observation systems for validation of atmospheric remote sensing

China Radiation Calibration Site (CRCS) is the first ground facility for calibration and validation of the remote sensing products in China. It started in the late 20th century and was aiming to obtain atmospheric status and ground reflectance for various series of satellites (Hu et al., 2001). Then in the next two decades, several observation networks for AC were established. These networks contributed significantly to validate satellite data products. In particular, China Aerosol Remote Sensing Network (CARSNET) (Che et al., 2016) and Sun/sky-radiometer Oberservation NETwork (SONET) were established for monitoring aerosol optical properties, while plenty of sites equipped with Multi-Axis Differential Optical Absorption Spectroscopy (MAX-DOAS) and other monitoring equipments built a network to monitor total column amounts and vertical profiles of trace gases. Moreover, an ozonesonde network led by the Institute of Atmospheric Physics (IAP), Chinese Academy of Sciences (CAS) has also been established to validate the ozone products. Besides, there were a few Chinese in-situ stations with ground-based Fourier Transform Spectrometers (FTS), which has become part of the Total Carbon Column Observing Network (TCCON) and provided precise and accurate measurements of the column-averaged dry-air mole fraction of atmospheric XCO_2.

The nation-wide ground-based observation network led by the China Meteorological Administration (CMA), namely CARSNET (as shown in Fig. 7), can obtain aerosol optical properties with high temporal resolution (Che et al., 2016). This network started in 2002 for dust aerosol monitoring and included 20 sites located in the northern and northwestern China. So far, it has been developed into the largest ground-based observation network of aerosol optical properties monitoring in China, consisted of 80 sites all over China, and more than 50 sites are running operationally (Che et al., 2011, Che et al., 2018, Zhao et al., 2018a). The ground gauges equipped in CARSNET sites are calibrated at least once a year to ensure the measurement accuracy. For the direct solar radiation, the calibration will be processed either by using the inter-calibrate method with reference to the master photometers at the site of Beijing-CAMS (Chinese Academy of Meteorological Sciences) or the Langley method at Mt. Waliguan Observatory (36.28°N, 100.09°E, 3816 m above sea level) (Che et al., 2009). In particular, the water vapor channel (936 nm) is calibrated following the modified Langley method (Che et al., 2016). After the periodical calibration with benchmark instruments, the AOD and water vapor content derived from CARSNET instruments differ by < 2% and < 5% relative to the master measurements, respectively. SONET is a joint network led by the Chinese Academy of Sciences and Chinese universities/institutes (as illustrated in Fig. 8), which extends CARSNET with multi-wavelength polarization measurement (CE318-DP) (Li et al., 2014). Many previous studies have confirmed that SONET could provide important in-situ calibration data for AOD derived from satellites (Li et al., 2019a;). Most recently, global 3.3 km high-resolution haze distribution from DPC/GF-5 was verified with 215 ground sites from AERONET and SONET. The results revealed a good consistency between DPC/GF5 and in-situ measurements (Ma et al., 2016).

MAX-DOAS retrieves tropospheric vertical profiles of trace gases and aerosols using scattered UV–vis sunlight measured at different elevation angles. The network currently contains 27 MAX-DOASs (Table 3), which are applied for the validation of satellite L2 products and investigation of a priori shape factor on the satellite retrievals (Wang et al., 2017a). This network mainly monitors NO_2, SO_2 and CH_2O. The sites are located in the North China Plain (NCP, including Beijing, Tianjin, Hebei, Shandong, Shanxi and Henan Provinces), the Yangtze River Delta (YRD, including Shanghai, Jiangsu and Anhui Provinces), the Great Bay Area (GBA, including Guangdong Province) and the Cheng-Yu region (including Chongqing and Sichuan Provinces). Moreover, two other instruments located at Ny-Ålesund in Arctic and at the Great Wall Station in Antarctica respectively are monitoring ozone, NO_2 and BrO. Observation of satellite EMI/GF5 has been verified using MAX-DOAS in Guangzhou Site (as illustrated in Fig. 9), and have shown that the Pearson correlation coefficient was 0.946 when the cloud cover was less than 0.3 (Zhao et al., 2018b).

Although the sparseness of ground-based observation leads to significant limitations in the detection of CO_2 in the atmosphere, the ground-based observation is still an indispensable part of the global CO_2 observation system. The Total Carbon Column Observing Network (TCCON) is a network of ground-based FTS recording direct solar spectra in the near-infrared spectral region, and its main goal is to provide precise and accurate measurements of the column-averaged dry-air mole fraction of atmospheric XCO_2, as well as other GHG (CH_4, CO) and trace gases (N_2O, H_2O, HDO, and HF) (Toon et al., 2009; Le et al., 2012; Buschmann et al., 2016; Kivi and Heikkinen, 2016). For example, the accuracy and precision of the XCO_2 measurements within TCCON is better than 0.25% (Wunch et al., 2011). There are four ground-based FTS sites in China (Table 4) as part of TCCON. Among these, the Beijing FTS site has been the first to provide XCO_2

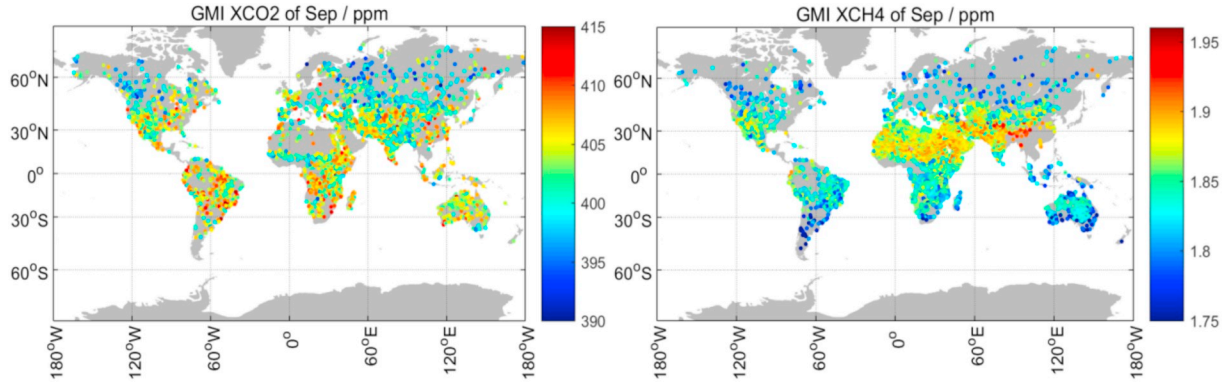

Fig. 6. Global distribution map of XCO_2 and XCH_4 column concentration from GMI in September 2018. The left panel and right panel are for XCO_2 and XCH_4, respectively.

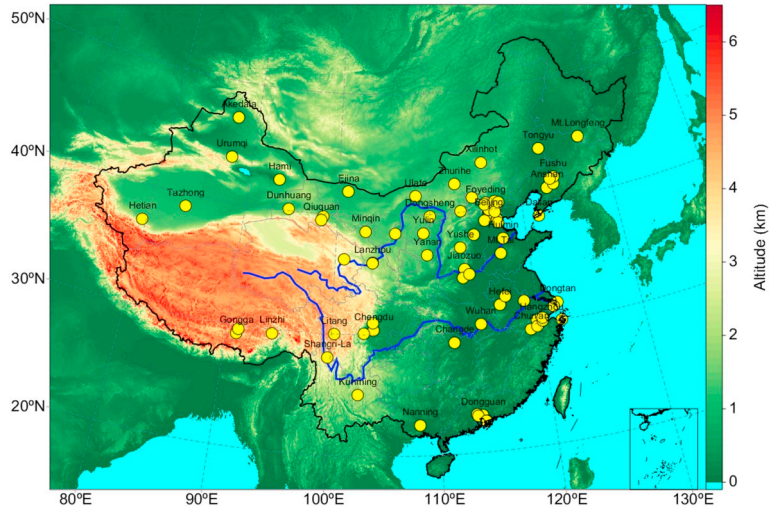

Fig. 7. Nation-wide distribution of China Aerosol Remote Sensing NETwork (CARSNET). The yellow dots denote the location of the 80 sites of CARSNET. (For interpretation of the references to colour in this figure legend, the reader is referred to the web version of this article.)

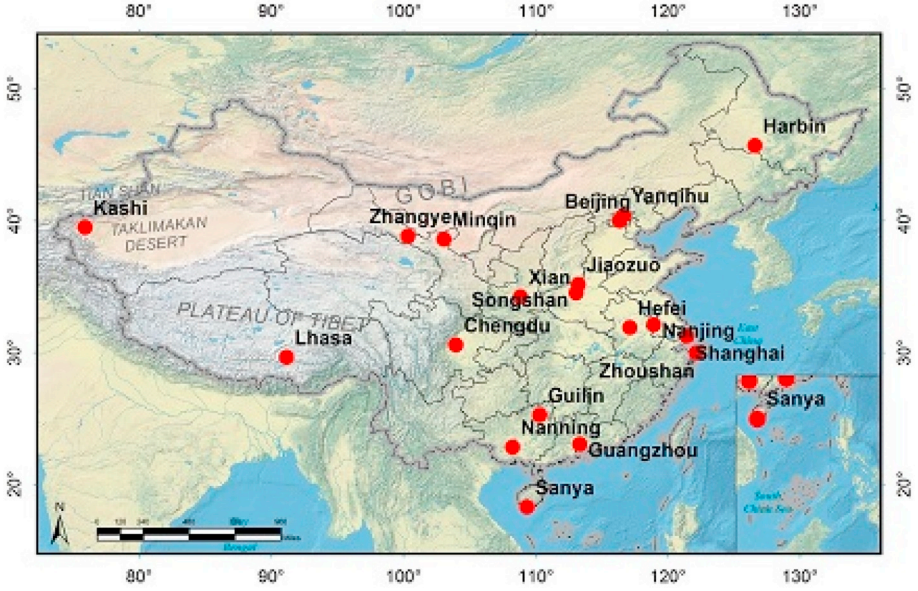

Fig. 8. Distribution of the stations as members of the Sun/sky-radiometer Oberservation NETwork (SONET). The red dots denote their locations. (For interpretation of the references to colour in this figure legend, the reader is referred to the web version of this article.)

observation since 1998 (Zhang et al., 2009b), while the other three sites, namely Heifei, Xinglong, and Xianghe, were all established in the 2010s. Studies based on observation of these sites are focused on the comparison at local scale, thus providing insight on assessments of the satellite measurements (Zhang et al., 2014; Zhou et al., 2015; Zhang et al., 2018; Meng et al., 2018; Zhou, 2018). As illustrated in Fig. 10, the correlation coefficient between GOSAT XCO_2 product and Beijing FTS is 0.88, with a positive bias of 1.35 ppm (Bi et al., 2018), while similar results with a correlation coefficient of 0.83 and a positive bias of 0.81 ppm are revealed by Wang et al. (2017b) in Hefei site. However, in comparison with OCO-2, XCO_2 products show a relatively lower correlation coefficient around 0.8 and a negative bias (Bi et al., 2018;). The observation data from these FTS sites can deep our understanding of the global climate through the validation of space-borne products.

3. Chinese future plans of atmospheric satellite missions

National Development and Reform Commission (NDRC) , Ministry of Finance (MOF) and Chinese National Space Administration (CNSA) have jointly released a strategic development plan of future satellite missions, including continuously strengthening space-borne observation of atmospheric composition, and particularly better evaluating aerosol, trace gases and GHG concentration in the atmosphere (National Development and Reform Commission NDRC et al., 2015). There are instruments included in the next FY-3 missions, while others are designed for thematic missions such as the second satellite of Gaofen-5 missions (GF-5(2)), Atmospheric Environmental Monitoring Satellite (AEMS) and High-precision Greenhouse gases Monitoring Satellite (HGMS).

FY-3E and FY-3G mission will add an advanced instrument, i.e. the Ozone Monitoring Suite (OMS), as the replacement of TOU/SBUS, while the GMI instrument will be onboard FY-3F and prolong operational monitoring for GHG. Besides, GF-5(02) with seven instruments onboard is planned to be launched in 2020. Compared with GF-5, GF-5(02) has an additional monitor to measure the AAI (Absorbing Aerosols Index). Both AEMS and HGMS are new pathfinders for atmospheric composition observation, which are planned to be launched in 2021 and 2023 respectively. Additionally, AEMS will be equipped with both active and

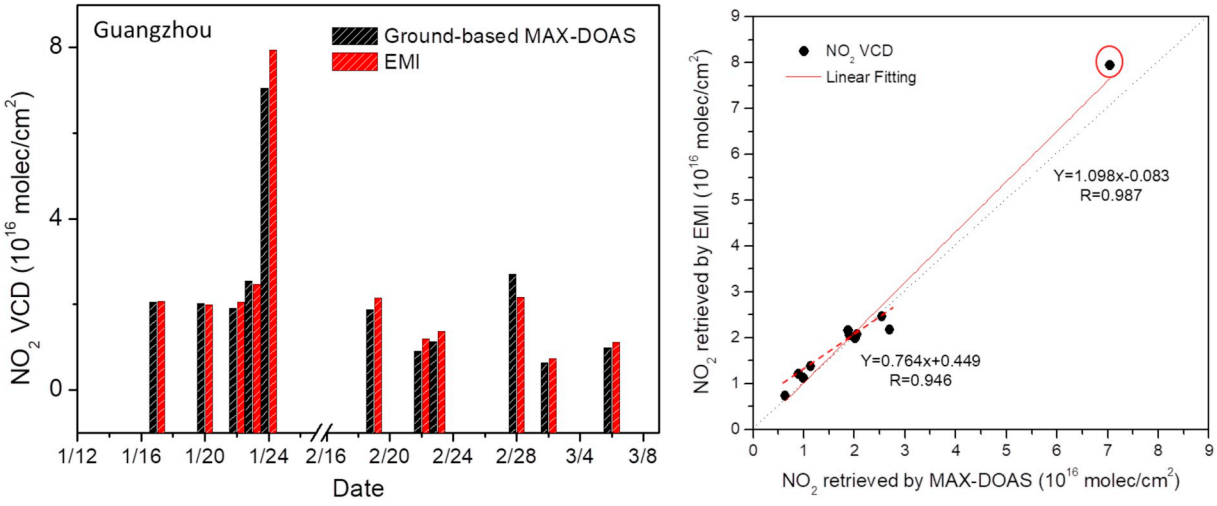

Fig. 9. Comparison of NO_2 columns by ground-based MAX-DOAS and EMI observations.

Table 4
Location of ground-based FTS sites in China.

Stations	Location	Year of operation
Beijing	39.955°N,116.334°E	1998
Heifei	31.90°N, 117.17°E	2014
Xinglong	40.40°N,117.59°E	2014
Xianghe	39.76 N, 116.98E	2018

passive instruments, aiming to measure particulate matters and air quality with high accuracy. AEMS is built on the similar platform as GF-5, and configured with five instruments, one active lidar, two polarimeters, one spectrometer and one land imager. Thus, active and passive instruments onboard HGMS will be aiming to measure GHG, such as CO_2 and carbon monoxide (CO). HGMS will be planed to carry an ultraviolet hyperspectral sounder, which has independent nadir and limb observation modules. The two modules can work simultaneously and obtain the horizontal and vertical distributions of pollution gases with high resolutions. HGMS is configured with five instruments, one active lidar, one polarimeter and three hyperspectral sounder. The orbit and LTAN (Local Time of the Ascending Node) of AEMS and HGMS are similar to GF-5. Thus these three missions can form the first Chinese satellite constellation specifically for AC monitoring.

4. Summary and conclusions

The second-generation Chinese polar meteorological satellites, namely FY-3, initiated the era of space observation for atmospheric composition. Since then, both the capability of the observing instruments and the relative calibration and validation techniques have been improved. However, before the FY-3A, few space missions were dedicated to monitor AC. Nevertheless, cameras onboard CBERS-1and HJ-1 could be used for monitoring air quality since the DT algorithm for AOD retrieval can be applied to their observation. The MERSI instrument onboard FY-3 can achieve global coverage of AOD in one day, while geostationary instrument AGRI onboard FY-4 could provide observations with high spatio-temporal resolutions. The first multi-angle polarized camera DPC equipped on GF-5 has enabled retrieval of aerosol properties, including types and sizes. Moreover, TOU and SBUS onboard FY-3 were the early instruments aiming to monitor ozone concentration, followed by EMI and AIUS onboard GF-5, which extended observation of trace gases. Thanks to their hyperspectral capabilities, ACGS/TanSat, GMI/GF-5 and GAS/FY-3D allowed retrievals of GHG, including tropospheric CO_2 and CH_4. Other than the space-borne part, the ground segments particularly the networks for the calibration and validation of AC products, have been established and they have contributed significantly to the correction of space-borne observation over mainland China.

The information provided by these observations and retrievals is valuable to understand a broad range of scientific questions, especially for monitoring the changes of climate and tracing the causes of air pollution events in China. Since the early studies concerned the evolution of stratospheric ozone, later investigations extended to atmospheric chemistry and dynamics due to the improvement of instrument

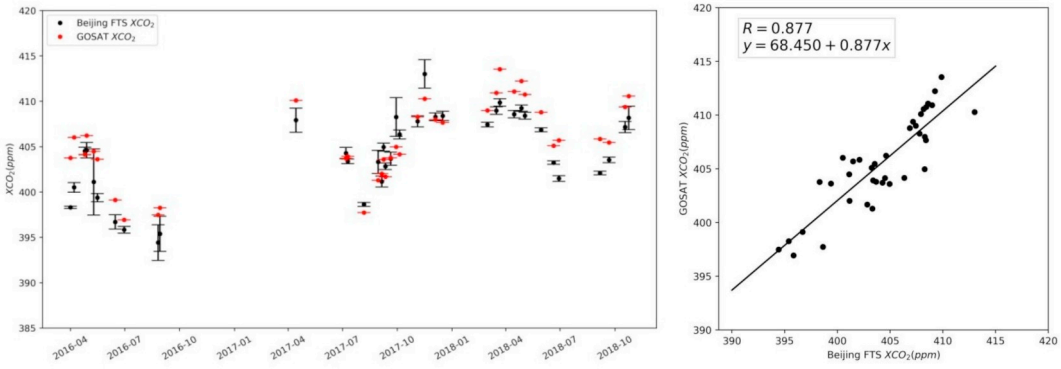

Fig. 10. Comparison of the averaged XCO2 between GOSAT and Beijing FTS. The left panel shows the time series of the XCO2 observation from GOSAT (red) and ground-based FTS in Beijing site (black). The right panel shows the correlation between the above mentioned observations. (For interpretation of the references to colour in this figure legend, the reader is referred to the web version of this article.)

capabilities. Further studies have provided substantial space-borne evidence for changes of atmospheric composition, and contributed significantly in assessing the impact of air quality policies and economic activities to air pollution trends, instead of on a local scale by from a global perspective.

Looking forward, the value of Chinese remote sensing satellites for monitoring AC can be further expanded by using cross-calibrated measurements from different instruments to develop a long-term, consistent data records. The long-term records of observations will help monitor the current and past global change of the earth's ecosystem. In the near future, through extending international cooperation to reduce possible instrumental uncertainty, a solid baseline could be established to prove the performence of in-orbit and future Chinese satellite missions, which then contribute more to the international community of AC monitoring.

Declaration of Competing Interest

The authors declare that they have no known competing financial interests or personal relationships that could have appeared to influence the work reported in this paper.

Acknowledgments

This work is supported by the National Key R&D Program of China (Grant Nos. 2017YFB0504001 and 2016YFB0500705) and the National Natural Science Funds of China (Grant Nos. 41775028 and 41601400).

References

Abad, G.G., Souri, A.H., Bak, J., Chance, K., Flynn, L.E., Krotkov, N.A., Lamsal, L., Li, C., Liu, X., Miller, C.C., Nowlan, C.R., Suleiman, R., Wang, H., 2019. Five decades observing Earth's atmospheric trace gases using ultraviolet and visible backscatter solar radiation from space. J. Quant. Spectrosc. Radiat. Transf. 19, 30107–30114.

Asher, E., Hornbrook, R.S., Stephens, B.B., Kinnison, D., Apel E.C., 2019. Using airborne observations to improve estimates of short-lived halocarbon emissions during summer from Southern Ocean. Atmospheric Chemistry and Physics 1–35.

Bao, Y.S., Zhu, L.H., Qin, G., Guan, Y.H., Lu, Q.F., Petropoulos, G.P., Che, H.Z., Ali, G., Dong, Y., Tang, Z.K., Gu, Y.J., Tang, W.Y., Hou, Y., 2019. Assessing the impact of Chinese FY-3/MERSI AOD data assimilation on air quality forecasts: sand dust events in Northeast China. Atmos. Environ. 205, 78–89.

Betts, A.K., Ball, J.H., Beljaars, A., Miller, M.J., Viterbo, P., 1996. The land surface-atmosphere interaction : a review based on observational and global modeling perspectives. J. Geophys. Res. 101 (3), 7209–7225.

Bi, Y.M., Wang, Q., Yang, Z.D., Chen, J., Bai, W.G., 2018. Validation of Column-Averaged Dry-Air Mole Fraction of CO2 Retrieved from OCO-2 using Ground-based FTS Measurements. J. Meteorol. Res. 32 (3), 433–443.

Bovensmann, H., Burrows, J.P., Buchwitz, M., Frerick, J., Noel, S., Rozanov, V.V., Chance, K., Goede, A.P., 1999. SCIAMACHY: Mission Objectives and Measurement Modes. J. Atmos. Sci. 56 (2), 127–150.

Bréon, F.M., Buriez, J.C., Couvert, P., Deschamps, P.Y., Deuzé, J.L., Herman, M., Goloub, P., Leroy, M., Lifermann, A., Moulin, C., Parol, F., Sèze, G., Tanré, D., Vanbauce, C., Vesperini, M., 2002. Scientific results from the Polarization and Directionality of the Earth's Reflectances (POLDER). Adv. Space Res. 30 (11), 2383–2386.

Burrows, J.P., Richter, A., Dehn, A., Deters, B., Orphal, J., 1999. Atmospheric remote-sensing reference data from GOME-2. Temperature-dependent absorption cross sections of O_3 in the 231-794nm range. J. Quant. Spectrosc. Radiat. Transf. 61, 509–517.

Buschmann, M., Deutscher, N.M., Sherlock, V., Palm, M., Thorsten, W., Justus, N., 2016. Retrieval of $_XCO_2$ from ground-based mid-infrared (NDACC) solar absorption spectra and comparison to TCCON. Atmos. Meas. Tech. 8 (10), 10523–10548.

Che, H.Z., Gui, K., Chen, Q.L., Zheng, Y., Yu, J., Sun, T.Z., Zhang, X.Y., Shi, G.Y., 2016. Calibration of the 936 nm water-vapor channel for the China aerosol remote sensing NETwork (CARSNET) and the effect of the retrieval water-vapor on aerosol optical property over Beijing, China. Atmos. Pollut. Res. 7 (5), 743–753.

Che, H.Z., Qi, B., Zhao, H.J., Xia, X.G., Eck, T.F., Goloub, P., Dubovik, O., Estelles, V., Cuevas-Agulló, E., Blarel, L., Wu, Y.F., Zhu, J., Du, R.G., Wang, H., Gui, K., Yu, J., Zheng, Y., Sun, T.Z., Zhang, X.Y., 2018. Aerosol optical properties and direct radiative forcing based on measurements from the China Aerosol Remote Sensing Network (CARSNET) in eastern China. Atmos. Chem. Phys. 18 (1), 405–425.

Che, H.Z., Wang, Y.Q., Sun, J.Y., 2011. Aerosol optical properties at Mt. Waliguan Observatory, China. Atmos. Environ. 45 (33), 6004–6009.

Che, H.Z., Zhang, X.Y., Chen, H.B., Damiri, B., Goloub, P., Li, Z.Q., Zhang, X.C., Wei, Y., Zhou, H.G., Dong, F., Li, D.P., Zhou, T.M., 2009. Instrument calibration and aerosol optical depth validation of the China Aerosol Remote Sensing Network. J. Geophys. Res.-Atmos. 114 (D3), 1–12.

Crutzen, P.J., 1979. The role of NO and NO_2 in the chemistry of the troposphereand stratosphere. Annu. Rev. Earth Planet. Sci. 7 (1), 443–472.

Dave, J.V., Mateer, C.L., 1967. A preliminary study on the possibility of estimating total atmospheric ozone from satellite measurements. J. Atmos. Sci. 24, 414–427.

Diner, D.J., Bruegge, C.J., Martonchik, J.V., Ackerman, T.P., Davies, R., Gerstl, S.A.W., Gordon, H.R., Sellers, P.J., Clark, J., Daniels, J.A., 1989. MISR: a multiangle imaging spectroradiometer for geophysical and climatological research from Eos. IEEE Trans. Geosci. Remote Sens. 27 (2), 200–214.

Dobber, M., Dirksen, R., Levelt, P.F., Gijsbertus, H.J., van den Oord, K.Q., Voors, R., Jaross, G., Kowalewski, M., 2006. Ozone monitoring instrument calibration. IEEE Trans. Geosci. Remote Sens. 44 (5), 1209–1238.

Dong, C., Yang, J., Zhang, W., Yang, Z., Lu, N., Shi, J., Zhang, P., Liu, Y., Cai, B., 2009. An overview of a new Chinese weather satellite FY-3A. Bull. Am. Meteorol. Soc. 90 (10), 1531–1544.

Eldering, A., Taylor, T.E., Odell, C.W., Pavlick, R., 2019. The OCO-3 mission: measurement objectives and expected performance based on 1 year of simulated data. Atmos. Measur. Techn. 12 (4), 1–54.

Flynn, L.E., Long, C.S., Wu, X., Evans, R., Beck, C.T., Petropavlovskikh, I., Mcconville, G., Yu, W., Zhang, Z., Niu, J., Beach, C., Sen, E., Hao, Y, Pan, C., Sen, B., Novicki, M., Zhou, S., Seftor, C.J., 2014. Performance of the ozone Mapping and Profiler Suite (OMPS) products. J. Geophys. Res. 119 (10), 6181–6195.

Ge, Q., Hu, Y.Q., Zhang, L., Zhang, S.M., 2017. Retrieval of Aerosol over Land Surface from FY-3C/MERSI with DDV Algorithm. Remote Sens. Inform. 32 (3), 34–38.

Gong, S.Q., Hagan, D.F.T., Lu, J., Wang, G.J., 2018. Validation of MERSI/FY-3A precipitable water vapor product. Adv. Space Res. 61 (1), 413–425.

Gong, S.Q., Hagan, D.F.T., Zhang, C.J., 2019. Analysis on Precipitable Water Vapor over the Tibetan Plateau using FengYun-3A Medium Resolution Spectral Imager Products. J. Sens. 1–12.

Gulde, S.T., Kolm, M.G., Smith, D.J., Maurer, R., Bazalgette Courrèges-Lacoste, G., Sallusti, M., Bagnasco, G., 2017. Knowing what we breathe: Sentinel 4: a geostationary imaging UVN spectrometer for air quality monitoring. In: Proc. SPIE. 10562. SPIE, pp. 1–9.

Guo, J.N., Yu, J., Zeng, Y., Xu, J.Y., Pan, Z.Q., Hou, M.H., 2005. Study on the relative radiometric correction of CBERS satellite CCD image. Science in China Series E Technological Science 48 (2), 12–28.

Han, W.H., Tong, L., Chen, Y.P., 2015. Aerosol Retrieval over Urban Area by Syngertic Use of Feng Yun-3C MERSI and Terra MODIS Data. In: 2015 *IEEE International Conference on Smart City/socialcom/sustaincom*. SmartCity 2015, pp. 108–111.

Hazem, T., 2019. Abd El-Hamid, Wenlong Wang, Qiaomin Li. Landscape Evaluation based on Gaofen Satellite in the Southern part of the Nile Delta, Egypt. Sci. Res. 7 (7), 47–60.

Heath, D.F., Krueger, A.J., Roeder, Henderson, B.D., 1975. The solar back-scatter ultraviolet and total ozone mapping spectrometer (SBUV/TOMS) for nimbus G. Opt. Eng. 14 (4), 323–331.

Herman, J.R., Hudson, R.D., Mcpeters, R.D., Stolarski, R.S., Ahmad, Z., Gu, X.Y., Wellemeyer, C., 1991. A new self-calibration method applied to TOMS and SBUV backscattered ultraviolet data to determine long-term global ozone change. J. Geophys. Res. 96 (4), 7531–7545.

Hu, X.Q., Zhang, Y.X., Zhang, G.S., Huang, Y.B., Wang, Y.K., 2001. Measurements and study of aerosol optical characteristics in China radiometric calibration sites. Quart. J. Appl. Meteorol. 12 (3), 257–266.

Huang, F.X., Liu, N.Q., Zhao, M.X., Wang, S.R., Huang, Y., 2010. Vertical ozone profiles deduced from measurements of SBUS on FY-3 satellite. Chin. Sci. Bull. 55 (10), 943–948.

Huang, F.X., Zhao, M.X., Yang, C.J., Dong, C.H., 2008. The retrieval algorithmof ozone profiles from measurements of Solar Backscatter UltravioletSounder (SBUS) on FY-3 satellite and its comparison retrieval trial. Prog. Nat. Sci. 18 (10), 1136–1142.

Huang, F.X., Huang, Y., Flynn, L.E., Wang, W.H., Cao, D.J., Wang, S.R., 2012. Radiometric calibration of the Solar Backscatter Ultraviolet Sounder and validation of ozone profile retrievals. IEEE Trans. Geosci. Remote Sens. 50 (12), 4956–4964.

Huang, C., Huang, F., Zhang, X., Lv, J., Cao, D., Liu, D., 2019. The possible responses of Polar ozone to Solar Proton events in March 2012 by FengYun-3 Satellite Observations. Space Weather- Int. J. Res. Appl. 17 (12), 1628–1638.

Hutchison, K.D., Cracknell, A.P., 2006. Visible infrared imager radiometer suite. Crc Press.

Ignatov, A., Petrenko, B., Kihai, Y., Stroup, J., Dash, P., Kramar, M., Gladkova, I., Liang, X.M., Zhou, X.J., Ding, Y.N., Huang, Y.X., Sapper, J., 2016. JPSS and GOES-R SST Products at NOAA. Amerfican Geophysical Union, 2016 Ocean Sciences Meeting. Amerfican Geophysical Union, Washington, DC, pp. 2407.

Kivi, R., Heikkinen, P., 2016. Fourier transform spectrometer measurements of column CO_2 at Sodankylä, Finland. Geosci. Instrument. Methods Data Syst. 5, 271–279.

Lacis, A., Hansen, J., Sato, M., 1992. Climate forcing by stratospheric aerosols. Geophys. Res. Lett. 19 (15), 1607–1610.

Le, K., Wunch, D., Shia, R.L., Connor, B., Miller, C., Yung, Y., 2012. Vertically constrained CO_2 retrievals from TCCON measurements. J. Quant. Spectrosc. Radiat. Transf. 113 (14), 1573–1761.

Li, Z.Q., Hou, W.Z., Hong, J., Zheng, F.X., Luo, D.G., Wang, J., Gu, X.F., Qiao, Y.L., 2018. Directional Polarimetric Camera (DPC): monitoring aerosol spectral optical properties over land from satellite observation. J. Quant. Spectrosc. Radiat. Transf. 218, 21–37.

Li, L., Li, Z., Li, K., Blarel, L., Wendisch, M., 2014. A method to calculate Stokes parameters and angle of polarization of skylight from polarized CIMEL sun/sky radiometers. J. Quant. Spectrosc. RA. 149, 334–346.

Li, C., Li, J., Xu, H., Li, Z., Xia, X., Che, H., 2019a. Evaluating VIIRS EPS Aerosol Optical Depth in China: an intercomparison against ground-based measurements and MODIS. J. Quant. Spectrosc. Radiat. Transf. 224, 368–377.

Li, Z.Q., Xie, Y.S., Hou, W.Z., Xu, H., Li, K.T., Li, L., Zhang, Y., 2019b. Global haze aerosol

distribution: a direct view by Geofen-5 satellite with 3.3 km spatial resolution. Atmospheric and Oceanic Physics 1–15.
Li, X.Y., Xu, J., Cheng, T.H., Shi, H.L., Zhang, X.Y., Ge, S.L., Wang, H.M., Zhu, S.Y., Miao, J., Luo, Q., 2019c. Monitoring trace gases over the antarctic using atmospheric infrared ultraspectral sounder onboard GaoFen-5: algorithm description and first retrieval results of O_3, H_2O, and HCl. Remote Sens. 11 (17), 1–18.
Li, Y.J., Xue, Y., He, X.W., Guang, J., 2012. High-resolution aerosol remote sensing retrieval over urban areas by synergetic use of HJ-1 ccd and modis data. Atmos. Environ. 46, 173–180.
Liang, Q.E., Susan, S.E., Fleming, E.L., 2017. Concerns for ozone recovery. Science 358 (6368), 1257–1258.
Liu, Y., Cai, Z.N., Yang, D.X., 2014. Effects of spectral sampling rate and range of CO2 absorption bands on XCO2 retrieval from TANSAT hyperspectral spectrometer. Chin. Sci. Bull. 59 (14), 1485–1491.
Liu, N.Q., Huang, F.X., Wang, W.H., 2011. Monitoring of the 2011 Spring low ozone events in the Arctic region. Chin. Sci. Bull. 56 (27), 2893–2896.
Liu, Y., Wang, J., Lu, Y., Chen, X., Cai, Z.N., Yang, D.X., Yin, Z.S., Gu, S.Y., Tian, L.F., Lu, N.M., Lyu, D.R., 2018. The TanSat mission: preliminary global observations. Sci. Bull. 63 (18), 38–45.
Liu, Y., Yang, D.X., Cai, Z.N., 2013. A retrieval algorithm for the Chinese carbon dioxide observation satellite TanSat: preliminary retrieval experiments using TANSO-FTS/GOSAT data. Chin. Sci. Bull. 58 (13), 1520–1523.
Lu, Q.F., Zhou, F., Qi, C.L., Hu, X.Q., Xu, H.L., Wu, C.Q., 2019. Spectral performance evaluation of high-spectral resolution infrared atmospheric sounder onboard FY-3D. Opt. Precis. Eng. 27 (10), 2105–2115.
Ma, Y., Li, Z.Q., Li, Z.Z., Xie, Y.S., Fu, Q.Y., Li, D.H., Zhang, Y., Xu, H., Li, K.T., 2016. Validation of MODIS Aerosol Optical Depth Retrieval over Mountains in Central China Based on a Sun-Sky Radiometer Site of SONET. Remote Sens. 8 (2), 111–124.
Manabe, S., Wetherald, R.T., 1980. On the distribution of climate change resulting from an increase in CO_2 content of the atmosphere. J. Atmos. Sci. 37 (1), 99–118.
Mei, L.L., Xue, Y., Guang, J., Li, Y.L., Wang, Y., Xu, H., He, X.W., Jiang, S.Z., Jiao, X.J., Chen, Z.Q., Ai, J.W., 2011. Aerosol optical depth retrieval over land using FY-3A data and its application in dust monitoring. Proceedings of SPIE - The International Society for Optical Engineering 8203 (5), 361–372.
Meng, X.Y., Zhang, X.Y., Zhou, M.Q., Bai, W.G., Zhou, L.H., Yu, X., Hu, Y.M., 2018. Validation and Analysis of GOSAT XCO2 Measurements by TCCON Sites. Meteorol. Monthly 44 (10), 1306–1317 (In Chinese).
Nakajima, M., Kuze, A., Suto, H., 2012. The Current Status of GOSAT and the Concept of GOSAT-2. Proceedings of SPIE-The International Society for Optical Engineering 8533 (24), 6–15.
National Development and Reform Commission (NDRC), Ministry of Finance(MOF), Chinese National Space Administration(CNSA), 2015. Medium and Long Term Development Strategy of China's Civil Space Infrastructure(2015–2025). Government Plan In Chinese.
Newman, P.A., Gleason, J.F., McPeters, R.D., Stolarski, R.S., 1995. Anomalously low ozone over the Arctic. Geophys. Res. Lett. 24 (22), 2689–2692.
O'Dell, C.W., Connor, B., Bösch, H., 2012. The ACOS CO2 retrieval algorithm-part 1: Description and validation against synthetic observations. Atmos. Measur. Techn. 5 (1), 99–121.
Pan, D.L., 2003. Satellite marine remote sensing in China. Proceedings of SPIE - The International Society for Optical Engineering 4892, 1–16.
Saide, P.E., Kim, J., Song, C.H., Choi, M., Cheng, Y., Carmichael, G.R., 2014. Assimilation of next generation geostationary aerosol optical depth retrievals to improve air quality simulations. Geophys. Res. Lett. 41, 9188–9196.
Salomonson, V.V., Barnes, W.L., Maymon, P.W., Montgomery, H.E., Ostrow, H., 1989. MODIS: Advanced facility instrument for studies of the Earth as a system. IEEE Transactions on Geoscience and Remoting Sensing 27 (2), 145–153.
Singh, A., Agrawal, M., 2007. Acid rain and its ecological consequences. J. Environ. Biol. 29 (1), 15–24.
Sun, Q., 2003. Technical Performance and Operational Mode of HY-1 a Satellite. Aerospace China 4, 12–14.
Sun, L., Sun, C.K., Liu, Q.H., Zhong, B., 2010a. Aerosol optical depth retrieval by HJ-1/CCD supported by MODIS surface reflectance data. Sci. China Earth Sci. 53 (S1), 74–80.
Sun, Z.P., Xiong, W.C., Wei, B., Li, Q., Wu, C.Q., Liu, X.M., 2010b. Image quality evaluation of HJ-1 satellite CCD sensor. Infrared (Monthly) 31 (9), 30–36.
Tang, W.Y., Bao, Y.S., Zhang, X.Y., Liu, H., Zhu, L.H., 2018. Comparison of FY-3A/MERSI, MODIS C5.1, C6 and AERONET aerosol optical depth in China. Acta Meteorol. Sin. 76 (3), 449–460 (In Chinese).
Taylor, T.E., O'Dell, C.W., O'Brien, D.M., 2012. Comparison of cloud- screening methods applied to GOSAT near-infrared spectra. IEEE Trans. Geosci. Remote Sens. 50 (1), 295–309.
Toon, G.C., Blavier, J.F.L., Washenfelder, R.A., Wunch, D., Keppel-Aleks, G., Wennberg, P., Cooner, B., Sherlock, V., Griffith, D., Deutscher, N., Notholt, J., 2009. Total Column Carbon Observing Network (TCCON). American Geophysical Union, pp. 1–10.
Veefkind, J.P., Aben, I., Mcmullan, K., Forster, H., Vries, J.D., Otter, G., Claas, J., Eskesa, H.J., Haana, J.F., Kleipoola, Q., Van Weelea, M., Hasekamp, O., Hoogeveen, R., Landgraf, J., Snel, R., Tol, P., Ingmann, P., Voorse, R., Kruizinga, B., Vink, R., Visser, H., Levelt, P.F., 2012. Tropomi on the esa sentinel-5 precursor: a gmes mission for global observations of the atmospheric composition for climate, air quality and ozone layer applications. Remote Sens. Environ. 120, 70–83.
Wang, X., Wang, G., Guan, Y., Chen, Q., Gao, L., 2005. Small satellite constellation for disaster monitoring in China. In: Proceedings. IEEE International Geoscience and Remote Sensing Symposium, 2005. IGARSS Seoul, South Korea.
Wang, Y., Beirle, S., Lample, J., Koukouli, M., Smedt, I.D., Theys, N., Li, A., Wu, D.X., Xie, P.H., Liu, C., Roozendael, M.VV., Thomas, W., 2017a. Validation of OMI, GOME-2A and GOME-2B tropospheric NO_2, SO_2 and HCHO products using MAX-DOAS observations from 2011 to 2014 in Wuxi, China: investigation of the effects of priori profiles and aerosols on the satellite products. Atmos. Chem. Phys. 17 (8), 5007–5033.
Wang, W., Tian, Y., Liu, C., Sun, Y.W., Liu, W.Q., Xie, P.H., Liu, J.G., Xu, J., Morino, I., Velazco, V.A., Griffith, D.W.T., Notholt, J., Warneke, T., 2017b. Investigating the performance of a greenhouse gas observatory in Hefei, China. Atmos. Measur. Techn. 10 (7), 2627–2643.
Wang, Z.T., Li, Q., Wang, Q., Li, S.S., Chen, L.F., Zhou, C.Y., Zhang, L.J., Xu, Y.J., 2012a. Hj-1 terrestrial aerosol data retrieval using deep blue algorithm. J. Remote Sens. 16 (3), 596–610.
Wang, W.H., Lawrence, F., Zhang, X.Y., Wang, Y.M., Wang, Y.J., Jiang, F., Zhang, Y., Huang, F.X., Li, X.J., Liu, R.X., Zheng, Z.J., Wei, Y., Liu, G.Y., 2012b. Cross-calibration of the total ozone unit (TOU) with the ozone monitoring instrument (OMI) and SBUV/2 for environmental applications. IEEE Trans. Geosci. Remote Sens. 50 (12), 4943–4955.
Wang, Z.T., Li, Q., Tao, J.H., Li, S.S., Wang, Q., Chen, L.F., 2009. Monitoring of aerosol optical depth over land surface using ccd camera on hj-1 satellite. China Environ. Sci. 29 (9), 902–907.
Wang, Q., Yang, Z.D., Bi, Y.M., 2014. Bi Yanmeng. Spectral parameters and signal-to-noise ratio requirement for Tansat hyper spectral remote sensor to measure atmospheric CO_2. J. Appl. Meteorol. Sci. 5, 600–609.
Wang, W.H., Zhang, X.Y., Wang, Y.M., Lu, J.G., Huang, F.X., Guan, F.J., Zhang, Z.M., Wang, J.H., Chen, J., Fu, L.P., 2011. Introduction to the FY-3A Total Ozone Unit(FY-3A/TOU): Instrument,Performance and Several Results. Int. J. Remote Sens. 32 (17), 4749–4758.
Wang, X., Zhao, D.Z., Su, X., Yang, J.H., Ma, Y.J., 2013. Retrieving precipitable water vapor based on fy-3a near-ir data. J. Infrared Millimeter Waves 31 (6), 550–555.
Winker, D., Pelon, M., 2003. J. The CALIPSO mission. 2003 IEEE International Geoscience and Remote Sensing Symposium. IEEE IGARSS 2, 1329–1331.
Wunch, D., Toon, G.C., Blavier, J.F.L., Washenfelder, R.A., Notholt, J., Connor, B.J., Griffith, D.W.T., Sherlock, V., Wennberg, P.O., 2011. The Total Carbon Column Observing Network. Philos. Trans. R Soc. (Math. Phys. Eng. Sci.) 369 (1943), 2087–2112.
Xia, X.L., Min, J.Z., Shen, F.F., Wang, Y.B., Yang, C., 2019. Aerosol Data Assimilation using Data from Fengyun-3A and MODIS: Application to a Dust storm over East Asia in 2011. Adv. Atmos. Sci. 36 (1), 1–14.
Xiong, W., 2018. Hyperspectral Greenhouse gases Monitor Instrument (GMI) for Spaceborne Payload. Spacecraft Recovery and Remote Sensing 39 (3), 14–24.
Xiong, W., 2019. Greenhouse gases monitoring Instrument(GMI) on GF-5 satellite (invited). Infrar. Laser Eng. 48 (3), 16–22.
Xu, Y.F., Li, Y.M., Wang, Q., Lu, H., Liu, Z.H., Xu, X., Tan, J., Guo, Y.L., Wu, C.Q., 2011. Eutrophication evaluation of three lakes and one reservoir using CCD images from the HJ-1 satellite. Acta Sci. Circumst. 31 (1), 81–93.
Yang, J., Dong, C.H., Lu, N.M., Yang, Z.D., Shi, J.M., Zhang, P., Liu, Y.J., Cai, B., 2009. FY-3A:the new generation polar-orbiting meteorological satellite of China. Acta Meteorol. Sin. 67 (4), 501–509.
Yang, Dongxu, Yi, Liu, Zhangnan, Cai, Xi, Chen, Lu, Yao, Lu, Daren, 2018. First global carbon dioxide maps produced from tansat measurements. Adv. Atmos. Sci. 35 (6), 621–623.
Zeng, Q.C., 1974. The Principle of Atmospheric Infrared Remote Sensing. Science Press, Beijing (in Chinese).
Zeng, Q.L., Wang, Z.F., Tao, J.H., Wang, Y.Q., Chen, L.F., Zhu, H., Yang, J., Wang, X.H., Li, B., 2017. Estimation of ground-level pm2.5 concentrations in the major urban areas of chongqing by using FY-3C/MERSI. Atmosphere 9 (1), 1–14.
Zhang, W.J., 2001. Status and Development of FY Series of Meteorological Satellites. Aerospace Shanghai 2, 8–14.
Zhang, X.Y., Meng, X.Y., Zhou, M.Q., Bai, W.G., Zhou, L.H., Hu, Y.M., Yu, X., 2018. Review of the validation of atmospheric CO2 from satellite hyper spectral remote sensing. Clim. Change Res. 14 (6), 60–70.
Zhang, Y., Wang, W.H., Li, X.J., Zhang, X.Y., Zheng, Z.J., Liu, R.X., 2012. Anomalously low ozone of 1997 Arctic spring: Monitoring results and analysis. Advances in Polar Science 23 (2), 82–86.
Zhang, X.Y., Zhang, P., Fang, Z.Y., 2007. Progress in trace gas remoting sensing study based on satellite monitorint. Meteorol. Monthly 33 (7), 3–14 (In Chinese).
Zhang, P., Yang, J., Dong, C., Lu, N., Yang, Z., Shi, J., 2009a. General introduction on payloads, ground segment and data application of Fengyun-3A. Front. Earth Sci. China 3 (3), 367–373.
Zhang, X.Y., Zhang, p., Liao, H., Hu, X.q., Li, Y., Zhang, L.J., Rong, Z.G., Qiu, H., 2009b. On Ground-based Remote Sensing for Atmospheric Species by FTIR Instrument and Retrieval Algorithm. Meteorol. Monthly 35 (1), 9–17.
Zhang, M., Zhang, X.Y., Liu, R.X., 2014. Study on the Validation of Atmospheric CO2 from Satellite Hyper Spectral Remote Sensing. Progressus Inquisitiones De Mutatione Climatis 10 (6), 427–432.
Zhang, X.Y., Zhou, M.Q., Wang, W.H., Li, X.J., 2015. Progress of global satellite remote sensing of atmospheric compositions and its' applications. Sci. Technol. Rev. 33 (17), 13–22 (In Chinese).
Zhang, P., Zhu, L., Tang, S., Gao, L., Chen, L., Zheng, W., Han, X., Chen, J., Shao, J., 2019a. General Comparison of FY-4A/AGRI with Other GEO/LEO Instruments and its potential and challenges in Non-meteorological applications. Front. Earth Sci. 6 (224), 1–13.
Zhang, P., Lu, Q.F., Hu, X.Q., Gu, S.Y., Yang, L., Min, M., Chen, L., Xu, N., Sun, L., Bai, W.G., Ma, G., Di, X., 2019b. Latest Progress of the Chinese Meteorological Satellite Program and Core Data Processing Technologies. Adv. Atmos. Sci. 36 (9), 1027–1045.

Zhao, H.J., Che, H.Z., Xia, X.G., Wang, Y.Q., Wang, H., Wang, P., Ma, Y.J., Yang, H.B., Liu, Y.C., Wang, Y.F., Gui, K., Sun, T.Z., Zheng, Y., Zhang, X.Y., 2018a. Multiyear Ground-based Measurements of Aerosol Optical Properties and Direct Radiative effect over Different Surface Types in Northeastern China. J. Geophys. Res.-Atmos. 123 (24), 13887–13916.

Zhao, M.J., Si, F.Q., Zhou, H.J., Wang, S.M., Jiang, Y., Liu, W.Q., 2018b. Preflight calibration of the Chinese Environmental Trace Gases Monitoring Instrument (EMI). Atmos. Meas. Tech. 11 (9), 5403–5419.

Zhou, M.Q., 2018. Retrieval of Carbon Dioxide and Other Greenhouse Gases from Ground-Based FTS Measurement and its Application. Chinese Academic Science & College of Earth Science Dissertation.

Zhou, C.Y., Bian, Z.J., He, Y.X., Li, Q., Liu, S.H., Zhao, S.H., Cheng, L.X., Yu, C., Chen, L.F., Wang, Z.T., Zhang, L.H., 2019. Introduction of GF-5 Satellite and Ability of monitoring NO_2 and O_3 Column Density from EMI. IGARSS 8796–8798.

Zhou, M.Q., Zhang, X.Y., Wang, P.C., Wang, S.P., Guo, L.L., Hu, L.Q., 2015. XCO2 satellite retrieval experiments in short-wave infrared spectrum and ground-based validation. Sci. China Earth Sci. 58 (7), 1191–1197.